Electrical and optical studies of gap states in self-assembled molecular aggregates

V. Burtman, G. Hukic, A. S. Ndobe, T. Drori, and Z. V. Vardeny[a)]
Department of Physics, University of Utah, Salt Lake City, Utah 84112

(Received 23 August 2006; accepted 4 January 2007; published online 2 March 2007)

We fabricated a variety of two-terminal devices using self-assembled monolayers (SAM) of solid-state mixtures comprised of molecular "wires" [1,4-methane-benzenedithiol (Me-BDT)] and molecular insulator "spacers" [1-pentanethiol], which were prepared at various molar concentrations ratio, r of wires/spacers, and sandwiched between two gold electrodes. The devices' electrical transport was investigated at several r values using the bias voltage (V) dependencies of the conductance and differential conductance at various temperatures. In parallel, we also studied the UV-visible absorption and photoluminescence (PL) emission spectra of the SAM mixtures grown on silica transparent substrates. For $r>10^{-3}$ we found that two-dimensional (2D) Me-BDT aggregates are formed in the SAM films leading to novel properties compared to SAM films of isolated Me-BDT molecules at concentrations $10^{-8}<r<10^{-4}$, which we studied before [V. Burtman, A. S. Ndobe, and Z. V. Vardeny, J. Appl. Phys. **98**, 034314 (2005)]. First, an Ohmic response in the current-voltage (I-V) characteristics is obtained up to $V\sim0.5$ V, which results in a new band in the differential conductance spectrum around $V=0$. Second, a new subgap absorption band is formed at $\sim$2.4 eV, which is related to a new yellow/red PL emission band. The novel optical and electrical properties of the 2D Me-BDT aggregates are explained by the formation of an electronic continuum band in the Me-BDT energy gap, which is caused by weak in-plane charge delocalization among the molecules forming the aggregates. To verify this model we also studied SAM molecular aggregate diodes using Al electrodes. The 1-eV difference in the electrode work function between Au and Al metals results in a pronounced E_F shift with respect to the aggregate-related continuum band in the gap, and consequently, dramatically changes the device I-V characteristics. © *2007 American Institute of Physics*. [DOI: 10.1063/1.2696401]

I. INTRODUCTION

Organic molecules with extended aromatic shells are natural quasi-one-dimensional (1D) systems for electrical transport. Such molecules were dubbed "molecular wires" due to the low value of the π-electron wave function decay constant, β, which is associated with large intramolecular electron conductance along the molecular principal axis. Starting with the first "single molecule" electronic device,[2] molecular electronics using such wire molecules has attracted tremendous interest in recent years. Currently, the most popular approaches of fabricating such 1D molecular diodes are mechanical break junctions,[2] electromigration break junctions,[3] films in nanopores,[4] nanoparticle bridged junctions,[5,6] and a broad range of devices in which scanning tunneling microscopy (STM) or atomic force microscopy (AFM) tips serve as the upper electrode.[7,8]

In two-dimensional (2D) macromolecular systems[9] the additional "dimension" is formed because of in-plane charge delocalization perpendicular to the molecular principal axis. This occurs, for example, in films of regioregular poly(3-alkyl-thiophene)[10] in which self-assembled lamella are formed perpendicular to the film substrate; and in molecular layer epitaxy structures.[11,12] Other ordered organic molecular systems also show delocalization perpendicular to the principal direction, but these are not strictly 2D. We mention, for example, single wall carbon nanotubes,[13] polyacetylene microcrystalline fibers,[14] and DNA double helix molecules.[15] Currently, the interest of charge and energy transport in 2D organic structures has increased mainly because of applications such as field-effect transistors involving π-conjugated polymers.

It is thus appealing to obtain a molecular engineering process that enables fabricating diodes of organic solid-state mixtures (SSM) with *controllable dimensionality* for systematic electrical transport studies of molecular organic devices with tunable dimensionality. This is analogous to inorganic semiconductor structures of which dimensionality can be presently controlled from three-dimensional (3D) (crystals) to 1D (quantum wires). We have recently introduced such a molecular engineering approach[1,16] using self-assembled monolayer (SAM) devices composed of molecular wires and insulator SSM. Using this approach we reported transport studies of SAM diodes having characteristic features of 1D isolated molecular wires. Similar molecular devices with 1D features were fabricated previously,[17,18] and interesting molecular transport properties were obtained.[19,20] However, there are only few reports of electrical transport through molecules at low temperatures. Also, no reports exist of studying transport in devices having controlled molecular wire densities. The ability of varying the molecular wire density in SAM devices is the most significant success of our novel

[a)]Author to whom correspondence should be addressed; electronic mail: val@physics.utah.edu

approach, and has enabled us to study here the novel transport properties caused by tuning the molecular wire density in the devices.

We fabricated two-terminal SAM devices and studied their electrical transport using the conductance and differential conductance dependencies on the bias voltage, V. We also investigated their optical properties using the absorption and photoluminescence (PL) spectra. We found that there are basically two r-value regimes of SSM SAM diodes: (i) $10^{-8} < r < 10^{-4}$, where the [1,4-methane-benzenedithiol (Me-BDT)] molecules are isolated in the [1-pentanethiol (PT)] insulator molecular matrix; and (ii) $10^{-3} < r$, where the Me-BDT molecules form 2D aggregates. In the isolated, well-dispersed, molecular wire regime we found that the electrical conductivity is dominated by electron transport through the molecular wires. The transport dramatically increases at where the electrode Fermi energy becomes resonant with the highest occupied molecular orbital (HOMO) level of the Me-BDT molecule. In molecular aggregates, however, we found that a second, high conductivity channel exists around $V=0$. This channel operates for $V < 0.5$ V, where the conductivity band in the differential conduction spectrum around $V=0$ V is obtained. In addition, the aggregates' SSM SAM films show a new double-peak absorption band in the Me-BDT optical gap that results in a yellow/red PL emission band. We speculate that the obtained band in the gap is due to new electronic states resulting from the molecular aggregation that form close to the Au Fermi energy. Indeed, when SSM SAM devices are fabricated using two Al electrodes with different work function and Fermi energy than those of Au electrodes, then the second transport channel does not occur around $V=0$ V, but rather at higher V that corresponds to the Fermi energy difference between Al and Au electrodes.

II. EXPERIMENTAL METHODS

A. SAM growth on Au electrodes

We used a molecular engineering approach in which SAM grows on metallic electrodes from solution mixtures of molecular wires (Me-BDT) and molecular insulating spacer molecules (PT) with a concentration ratio, $r = N_{\text{Me-BDT}}/N_{\text{PT}}$, where $N_{\text{Me-BDT}}$ and N_{PT} are their respective molar concentrations. Our goal has been to fabricate SSM SAM devices with predictable structural features, where the isolated molecular wires are well dispersed in the insulated matrix of aliphatic molecules having "dielectric" properties. SAM devices were fabricated using the protocol shown schematically in Fig. 1 for large r values.

The bottom Au electrode (about 30 nm thick) was deposited on a SiO_2/Si wafer using a DVSJ/20C Denton Vacuum e-gun. The Me-BDT and PT precursors' mixture was diluted with distilled toluene to 3-mM solution, and transferred to a homemade high-vacuum-based Shlenk line. The self-assembling process continued for about 12 h in an argon atmosphere at room temperature. When the self-assembly process was completed the samples were thoroughly washed in dry toluene and annealed in vacuum for 1 h at 90 °C for removing possible physisorbed precursors. The upper Au electrode was then evaporated through a shadow mask in a vertical cross-electrodes configuration [Figs. 1(c) and 1(d)] using a DV-SJ/20C e-gun at 95 °C on the sample holder. During the self-assembly process we varied the stoichiometric ratio, r, in the range $10^{-8} < r < 1$. For our two-terminal devices the Si chip contained three different devices, each of them with an active area of about 0.5 mm^2. The device measurement concept is depicted in Fig. 1(d).

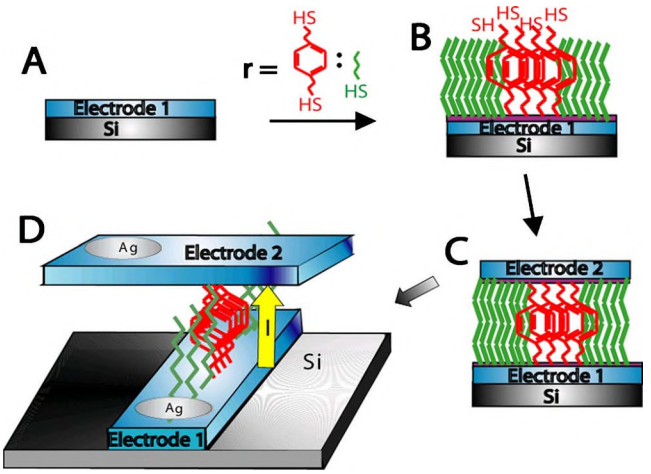

FIG. 1. (Color online) The fabrication process (schematic) of SAM solid state mixture diodes at large ratio, r of molecular wires (Me-BDT in red) to molecular insulators (PT in green) for transport studies. (a) Evaporation of the base electrode; (b) SAM growth of the appropriate solid state mixture on the bottom electrode; (c) evaporation of the upper electrode; (d) I-V measurement setup.

Due to different molecular growth rates in the self-assembly process, the ratio of the wire/insulator molecule density in the SAM configuration may not be equivalent to the stoichiometric ratio r in the solution. We assume that the wire and insulator molecules form SSM in the monolayer, which is characterized by the nominal r value from the solution mixtures. The actual density of the molecular wires was determined by a surface titration method, as described in Ref. 16. Changing the r value in the solution thus tuned the conduction mechanism from the regime of isolated Me-BDT molecules ($10^{-8} < r < 10^{-4}$) to the regime of 2D molecular aggregates for $r > 10^{-3}$, which is in the scope of the present work.

The Me-BDT molecule has two thiol groups, one at each end, whereas the insulating PT molecule has only one such thiol end group. The thiol group in molecular electronics is considered to be a "molecular alligator" due to its ability to form a sulfide bond with metal electrodes. Usually, bonding is an indispensable condition for obtaining Ohmic contacts with the metal electrodes. The absence of one thiol group in the PT molecule forms a "spatial gap" between the molecule and upper electrode. In other words, Me-BDT can bond to both electrodes via sulfur-metal bonding, and thus has relatively high conductance. PT molecules, however, bond only to one electrode, and this leads to very low electrical conductivity.[1,16]

B. Initial characterization of the Me-BDT/PT monolayers

The step-by-step growth of the organic monolayers was characterized by contact angle changes, *ex situ* ellipsometry,

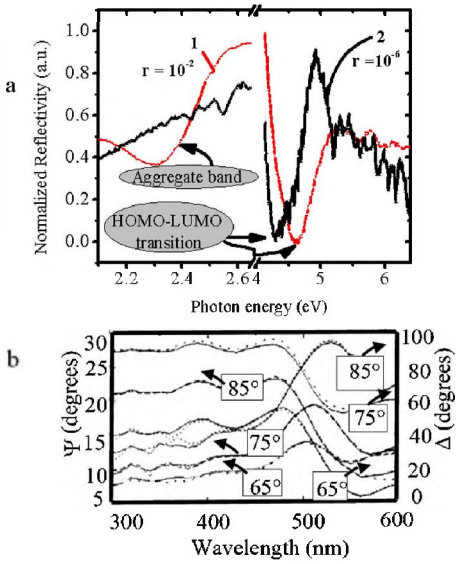

FIG. 2. (Color online) Basic optical measurements of the fabricated SAM devices. (a) The optical reflectivity spectrum of SAM films with $r=10^{-2}$ (red dashed line, 1), and $r=10^{-6}$ (black solid line, 2) that show a prominent feature at the HOMO-LUMO transition of the Me-BDT molecule at about 5 eV. For $r=10^{-2}$ there is another optical feature in the visible spectral range associated with Me-BDT aggregates. (b) Ellipsometry spectra of two optical constants: ψ (dashed line) and Δ (dotted line) that were measured at three different angles, from which a film thickness of ~1 nm was derived. The solid lines through the data points are model fittings (see text).

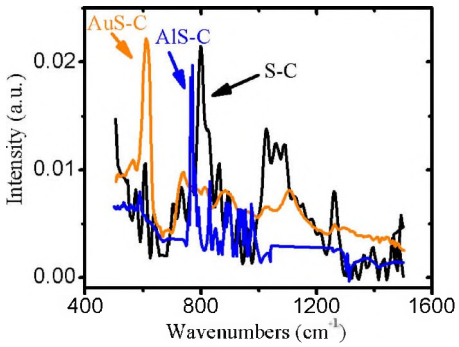

FIG. 3. (Color online) FTIR absorption spectra of Me-BDT molecules bonded to the upper electrode that show the IR-active stretching vibration of various metals bonded to the sulfur atom of the molecule: orange line is for AuS-C vibration; and blue line: AlS-C. For reference the black line is for the S-C stretching vibration.

and UV-visible (UV-vis) reflectance spectroscopy; these are briefly summarized in Fig. 2. After step "A" in Fig. 1, the contact angle changed from 17° to 45°, and the UV-vis reflectivity spectrum of the film grown on the Au/Si substrate [Fig. 2(a)] shows a 281-nm peak characteristic of the Me-BDT molecule HOMO to lowest unoccupied molecular orbital (LUMO) transition. We note that the HOMO-LUMO transition in the Me-BDT aggregates is blueshifted by ~20 nm, to 261 nm, with respect to that of the isolated molecules.[1] Moreover, the visible part of the optical reflectivity spectrum reveals a new characteristic transition of Me-BDT molecular aggregates that is only present at large r values. This was taken as evidence that Me-BDT molecules form aggregates for SAM of $r>10^{-3}$.

Variable angle spectroscopic ellipsometry (Woollam Co.) was used to verify the monolayer growth in the device structure [Fig. 2(b)].[16] This method measures the optical spectra in the visible spectral range of 300–600 nm with 5 nm resolution. The structural model for fitting the *ex situ* ellipsometry data uses the collected data from three different incident angles, namely, 65°, 70°, and 75°. The obtained ellipsometric spectra for the structures containing Si/SiO_2, Au, and Me-BDT/PT monolayers exhibit molecular c-axis interplanar spacing of ~30 nm for the bottom Au film, and ~10 Å for the monolayer of Me-BDT/PT SSM. This indicates that single organic monolayer growth is achieved.

C. SAM two-terminal Au and Al devices

Gold electrodes are best for high-quality SAM diodes since they are less prone to oxygenation compared to Al electrodes; thus, most of our studies were performed on Au-SAM-Au diodes. Nevertheless, we also studied devices with Al electrodes. Alkanethiol can, in principle, attach to any metal surface that is covered by an oxide layer,[21,22] via a two-step reaction. First, the thiol moiety dissolves the oxide layer; this is followed by a metal-sulfur bond. Al-SAM-Al devices were fabricated using the same synthetic protocol as for Au electrodes described above, but in an inert atmosphere to avoid oxidation. In addition, the electrode deposition process for both upper and lower electrodes was done in a glove box.

D. Checking molecular connectivity of the SAM diodes

Bonding of the self-assembled molecules to the bottom electrode was well characterized in previous studies of thiol-ended SAM on various metals.[23] The assembled molecules interact on the surface via van der Waals forces between adjacent alkyl chains. As a result of the intrinsic stability of such systems, SAM grown on metallic films is known to have low defect density, and also resists degradation in air.[24]

In contrast, the connectivity with the upper electrode is an acute problem in the field of molecular electronics.[25] To address the formation of covalent bonds between the Me-BDT molecules in the SAM devices and the upper electrodes, we fabricated SAM structures comprised of *iodopropyl-trimethoxysilane* self-assembled onto a SiO_2/Si film. This was followed by chemisorption of either a Me-BDT monolayer or a PT monolayer that was used as a control structure. We used the silane matrix as a template layer for the SAM since it is semitransparent in the mid-IR spectral range and this allows for absorption spectroscopy study of the upper surface vibrational modes. Using these structures we confirmed the bonding with the upper electrodes by studying the stretching vibration frequency of the C-S-metal bond for Au and Al electrodes. Upon deposition of the upper electrode Au-S bonds are indeed formed, and this is detected via IR absorption since the frequency of the IR-active Au-S stretching vibration is different from that of the original C-S stretching vibration (before metal deposition)[26] (Fig. 3). In fact, the IR-active vibration frequency shifts from ~798 cm^{-1} (Fig. 3, black line) for the C-S stretching mode, to ~614 cm^{-1} (Fig. 3, orange line) for the Au-S-C mode. The redshifted IR-active vibration mode was absent in the con-

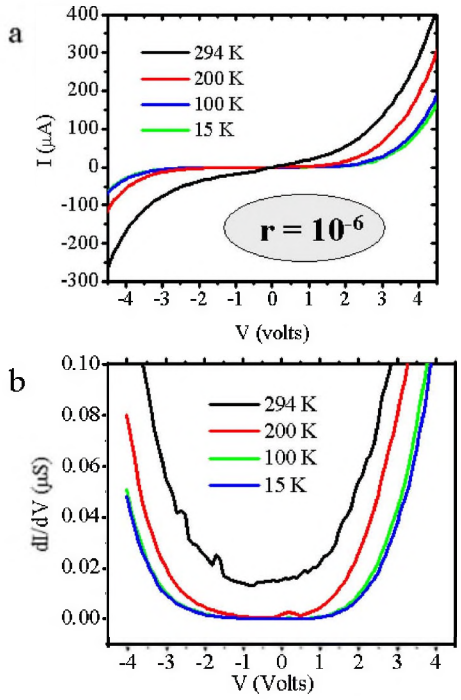

FIG. 4. (Color online) Electrical transport measurements of SAM diodes with $r=10^{-6}$ at various temperatures, showing isolated Me-BDT behavior. (a) *I-V* characteristics; (b) differential conductance spectrum obtained from (a).

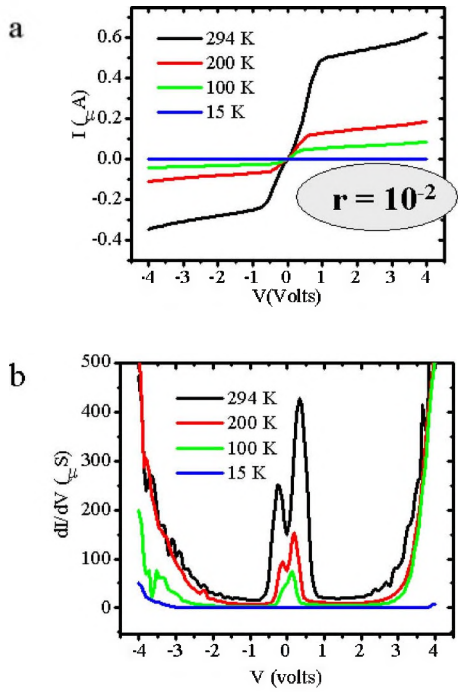

FIG. 5. (Color online) Electrical transport measurements of SAM diodes devices with $r=10^{-2}$ at various temperatures showing Me-BDT aggregates behavior. (a) *I-V* characteristics; (b) differential conductance spectrum obtained from (a).

trolled structure that contained only PT molecules, confirming that these molecules do not bond with the upper Au electrode. The Al-S-C stretching vibration mode also redshifts (Fig. 3, blue line) compared to the C-S stretching mode frequency; however, the shift for Al is only 28 cm^{-1}, compared to 184 cm^{-1} for Au.

III. EXPERIMENTAL RESULTS AND DISCUSSION

A. Transport studies of Au/SAM/Au diodes

We studied the transport properties of the fabricated molecular diodes at various temperatures by measuring the characteristic current-voltage (*I-V*) dependence, as well as the differential conductance spectrum (DCS) ($=dI/dV-V$); these are shown in Fig. 4 ($r=10^{-6}$) and Fig. 5 ($r=10^{-2}$). All temperature-dependent conductivity measurements were performed under a dynamic vacuum.

For reference, we first discuss the conductivity measurements of a device with $r=10^{-6}$ (Fig. 4), at r value in the range where the Me-BDT molecular wires are isolated in the otherwise insulating PT matrix. The transport process in this device is dominated by tunneling through the HOMO-E_F barrier that is formed between the Me-MDT HOMO and the Au electrode Fermi energy, E_F(Au). This is apparent in Fig. 4(b), where the DCS spectrum is plotted at four different temperatures. The 15-K data (that do not contain any thermionic contribution) show an abrupt change at a voltage onset, $V(\text{on})\sim 2.4$ V. This occurs when E_F reaches resonance with the Me-BDT HOMO level. We may estimate the energy difference, Δ_{BDT} between E_F and Me-BDT HOMO level from $V(\text{on})$ using the relation[1] $V(\text{on})=2\Delta_{\text{BDT}}/e$; accordingly, we get $\Delta_{\text{BDT}}\sim 1.2$ eV. This value is much smaller than the Me-BDT HOMO-LUMO gap, which we estimate from the optical measurements in Fig. 3 to be ~4.4 eV (Ref. 1). This verifies that E_F(Au) lies inside the Me-BDT HOMO-LUMO gap.[27]

For devices where molecular wire aggregates are formed ($r\geq 10^{-3}$) we observed a new transport channel [Figs. 5(a) and 5(b)] as well as novel optical features [Figs. 2(a)], which are related to the formation of new states in the Me-BDT HOMO-LUMO gap. Upon Me-BDT aggregation the injected charges may move in plane, in addition to the preferred direction along the molecular axis. As is apparent in Fig. 5(a) the *I-V* response of such a device is much steeper at low V compared to that of devices with isolated Me-BDT molecules [Fig. 4(a)], and also shows much higher conductivity. Moreover, a new feature appears in the DCS spectrum at $V<0.8$ V, in addition to the DCS tunneling features characteristic of the isolated Me-BDT molecules seen at higher V (at ~3 V). Specifically, the *I-V* response at $V<0.8$ V appears to be linear, with some nonlinearity in the vicinity of $V=0$ [Fig. 5(a)]. This new *I-V* feature produces a peak in the DCS spectrum at low temperature for $V<0.8$ V [Fig. 5(b)]. For $V>1$ V the additional DCS aggregate-related band diminishes and turns back to that of typical tunneling through SAM molecules seen in isolated molecule devices at high V discussed above [Fig. 4(b)].

B. The formation of gap states in aggregated Au/SAM/Au devices

For explaining the novel DCS feature around $V=0$ in aggregated SAM devices we consider that a relatively narrow continuum band (COB) of molecular orbitals is formed inside the Me-BDT HOMO-LUMO gap due to the in-plane

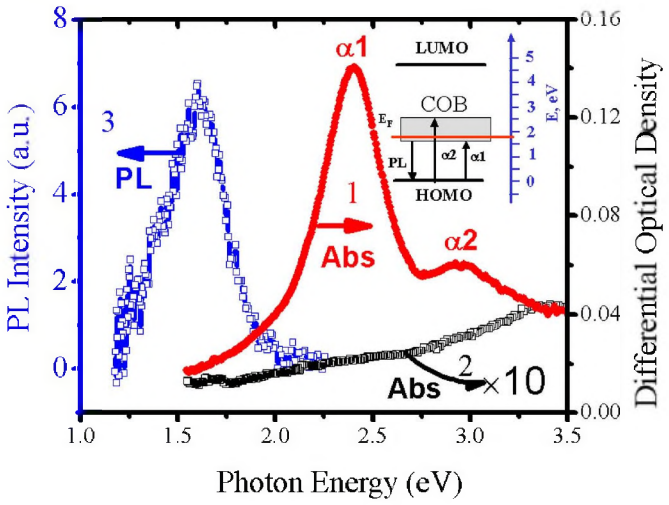

FIG. 6. (Color online) Room temperature differential optical density spectra of SAM films with $r=10^{-2}$ (red squares) and $r=10^{-4}$ (black squares) obtained using semitransparent Au electrodes and sapphire substrates, respectively. The SAM film with $r=10^{-2}$ shows two absorption bands (α_1 and α_2) that indicate aggregate formation; as well as a PL emission band (blue dots). The insert shows schematically the gap states (COB) in the Me-BDT HOMO-LUMO gap that are formed for aggregated SAM. α_1 and α_2 transitions, the gap state COB, and the PL process are assigned; and the gold Fermi level, E_F(Au) is shown respect to the COB at $V=0$.

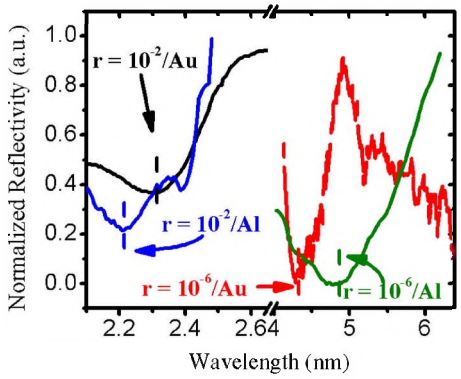

FIG. 7. (Color online). Normalized optical reflectivity spectra of SAM films on Au and Al electrodes, respectively, at two r-values: (i) $r=10^{-6}$ for isolated Me-BDT; and (ii) $r=10^{-2}$ for molecular aggregates. The Me-BDT HOMO-LUMO transition at ~4.5 eV, and the optical transition related to Me-BDT aggregates at ~2.3 eV are assigned.

π-electron stacking. This is analogous to the well-known narrow impurity band formed in heavily doped semiconductors caused by overlapping nearest-neighbor orbitals, for example, a phosphorous impurity band in heavily n-type silicon doping.[28,29] If the molecular COB lies close to E_F(Au) then an abundance of dense molecular levels are available for electron transport, and consequently, this would dramatically enhance the electrical conductivity (Fig. 6, inset). In this case, a low interface barrier potential would form between the metal electrode and the aggregate-related COB, similar to the case of a metal/heavily doped-semiconductor (SEC) interface in metal/SEC/metal devices.[30]

With this simple model we can explain the transport characteristic properties obtained in aggregated SAM devices. We infer the existence of a very efficient transport mechanism in the voltage range in which E_F(Au) is aligned with the molecular COB in the gap. In this model both I-V and DCS at low V are dominated by carrier injection into the molecular COB. The in-gap COB is scanned upon ramping V, and at $V=V_{max}\sim 0.8$ V E_F(Au) is no longer aligned with the COB band in the gap, because the aggregate-related COB is quite narrow, typically ~0.5 eV. Consequently, the I-V and DCS spectra for $V>V_{max}$ again exhibits the usual tunneling features typical for isolated molecular wires; specifically, the conductivity increases again at V where E_F(Au) becomes aligned with the Me-BDT molecular HOMO level, as in SAM devices with $r<10^{-4}$.

During the self-assembly growth (step "A" in Fig. 1) the UV-vis reflectivity spectrum shows a strong, 286-nm band characteristic of the HOMO-LUMO optical transition for the isolated Me-BDT molecules [Figs. 6(a) and 2(a)]. Whereas the visible part of the optical reflectivity spectrum is featureless for devices with isolated molecular wires, a new optical transition with a peak at ~2.3 eV is observed in aggregated devices at large r values [$r>10^{-2}$; Fig. 6(a)]. Moreover, this new band was found to be optically active, and upon excitation at 2.4 eV it produces an associated PL emission band with a maximum at ~1.6 eV. This validates the assumption that the Me-BDT molecules are indeed aggregated in the 2D SAM devices for $r>10^{-3}$. The apparent peak, α_1 (~2.4 eV), and shoulder, α_2 (~2.9 eV), in the absorption spectrum [Fig. 6(a)] may actually probe the bottom and upper electronic levels of the aggregate-related COB density of states in the gap. Remarkably the COB detected by optics (Fig. 6) has the same width (~0.5 eV) as the DCS band around $V=0$ detected by transport [Fig. 5(b)].

C. Gap states in Al/SAM/Al devices

1. Optical studies

We measured the optical reflectivity spectra of SAM films on Al electrode with the same r values as were used for devices with Au substrates [Fig. 2(a)]. In particular, for a SAM with $r=10^{-6}$ self-assembled molecular wires on Au (Fig. 7, red curve) shows a prominent spectral feature at ~280 nm that corresponds to the HOMO-LUMO transition of the isolated Me-BDT molecules on Au substrates. Self-assembled wire molecules on Al substrates, however (Fig. 7, olive curve), exhibits a blueshift of the HOMO-LUMO transition to ~260 nm. This blueshift might be explained by a different electrostatic environment for different metallic substrates. SAM films with $r=10^{-2}$ on Al substrates (Fig. 7, blue curve) also show a new aggregate-related spectral feature in the visible spectral range ~560 nm, similar to that on Au substrates. This absorption band is absent in self-assembled isolated wires on Al substrates. The absorption band is redshifted compared to that of aggregated SAM on Au substrates, which occurs at ~525 nm; nevertheless, it has the same width. We thus believe that it originates from the same process, namely Me-BDT aggregates. We attribute the shift of the aggregate-related band to different macroscopic structures of SAM on these two metallic surfaces. The aggregates may form a larger domain size, and this may result in a broader and lower energy band with the Al substrates. It is well known that SAM of similar molecules on different substrates may result in different packing.[31] UV and inverse

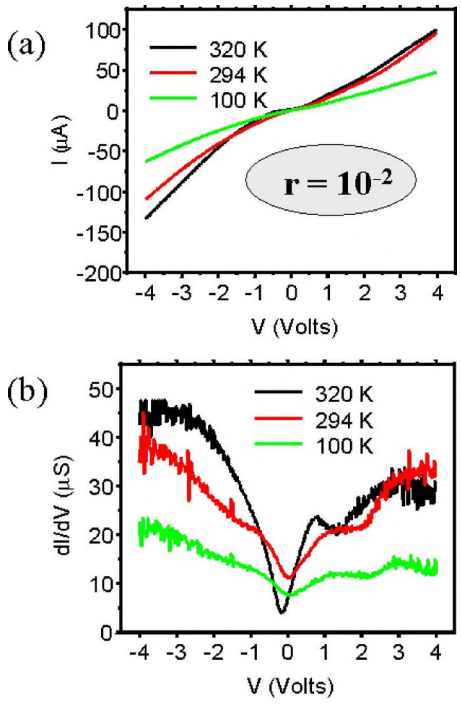

FIG. 8. (Color online) Electrical transport measurements of aggregated SAM diodes having $r=10^{-2}$ with Al electrodes (Al-SAM-Al) at various temperatures. (a) I-V characteristics; (b) differential conductance spectrum obtained from (a).

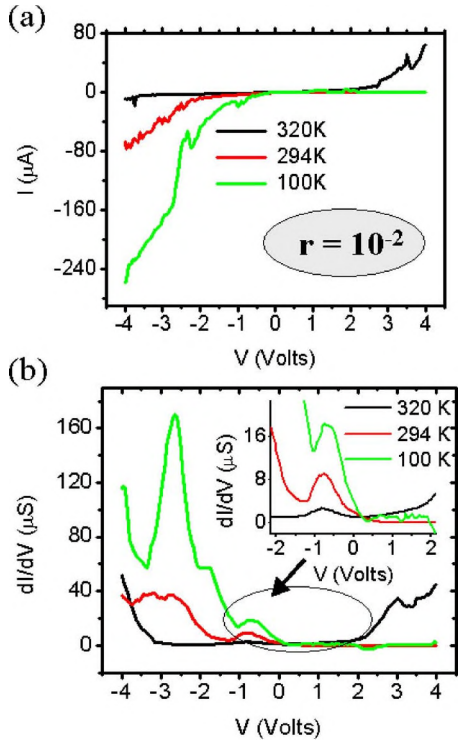

FIG. 9. (Color online) Same as in Fig. 8 but for a SAM diode with bottom Al and upper Au electrodes (Au-SAM-Al). The insert in (b) shows an expanded version of the low bias data.

photoemission spectroscopies, as well as x-ray photoemission spectroscopies (XPS) studies, would be required to determine the reason of the spectroscopic differences between aggregated SAM on Au and Al electrodes. However, we take these experimental facts as an indication of aggregate formation in SSM on Al substrates, similarly to aggregate formation on Au substrates at large r values.

2. Transport studies

The I-V and $dI/dV-V$ characteristics of the aggregated Al/SAM/Al and Au/SAM/Al diodes at $r=10^{-2}$ at different temperatures are summarized in Figs. 8 and 9, respectively. Remarkably, the I-V curves of aggregated Al/SAM/Al diodes at large r value [Fig. 8(a)] seem to be similar to the I-V curves of isolated wire Au/SAM/Au devices seen at small r value, in that the DSC spectra do not reveal a new band at low V [Fig. 8(b)]. This is despite the fact that the spectroscopic data *indeed show* the existence of aggregate-related COB in the gap for the same SAM film. We argue that this seeming paradox is due to the shift of E_F(Al) with respect to the aggregate-related COB energy in the gap.

It is known from electrode work-function studies in organic devices that E_F(Al) is shifted with respect to E_F(Au) by about 1 eV (Ref. 32). The energy alignment of Al and COB in the molecular gap is depicted in the inset of Fig. 6(a). It is seen that E_F(Al) is therefore not aligned with the aggregate-related COB in the gap at $V=0$. As a matter of fact, E_F(Al) is *above* the COB in Me-BDT aggregates. Consequently, ramping V does not result in E_F(Al)-COB crossing at V smaller than that of the HOMO-E_F barrier. This situation is similar to textbook examples of transport features seen in inorganic semiconductor structures, where transport is suppressed at some V range due to lack of available electronic states in the structure at some energy interval, which may lead to negative resistance or negative conductivity devices.

In a control experiment we compare the transport of aggregated Al/SAM/Al with Au (upper)/SAM/Al (bottom) diodes (Fig. 9). Based on our model above we expect that E_F(Au) would align with COB, whereas E_F(Al) would not. Due to the electrodes work-function difference we expect a built-in potential of $\sim$1 eV in such molecular diodes. We indeed obtained such asymmetry of the aggregated Au (upper)/SAM/Al (bottom) I-V curve [Fig. 9(a)] with a "zero shift" of $\sim$1 V with respect to the Au/SAM/Au device. We also obtained a low-energy band in the DCS [Fig. 9(b)] that is characteristic of COB in aggregated devices, only when current is injected from the Au electrode (i.e., $V<0$). At the same time we do not obtain such a feature when current is injected from the Al electrode ($V>0$). This control experiment validates our working model of COB formation in the aggregate SAM devices.

IV. CONCLUSIONS

We studied SAM diodes based on two-component solid-state mixtures of molecular wires (Me-BDT) and insulators (PT) at various molar ratio, r. This approach enables the fabrication of molecular devices with 1D response at low r values ($r<10^{-4}$), where the isolated molecular wires dominate transport[1,16]; along with devices based on 2D response at higher r-values ($r\geq 10^{-3}$), where the Me-BDT molecules form surface aggregates. The electrical transport characteristics of SAM diodes fabricated with Au and Al electrodes

were investigated via *I-V* and DCS dependencies on *V*, at various temperatures; and by optics, including UV-vis is absorption and PL emission spectra.

The transport characteristics properties of 2D molecular diodes at high *r*-value were modeled within the weak charge delocalization approach. We postulate the existence of new gap states in the Me-BDT HOMO-LUMO gap that form a continuum band (COB) due to the aggregation, at ~2 eV above the HOMO level. The aggregate-related COB is formed in the gap at roughly the same energy as the gold Fermi level. This model explains the low energy features in the *I-V* and $dI/dV-V$ spectra of Au/SAM/Au diodes, as well as the new absorption bands and associated PL emission band.

To verify our working hypothesis we also studied SAM diodes based on Al and Al-Au electrodes combination. The difference in the work-function values between Au and Al metals is ~1 eV, and thus it is expected that a corresponding difference in E_F between these two metal electrodes respect to COB should influence the device transport response. We indeed found that the transport features that were attributed to COB in Me-BDT aggregates in Au/SAM/Au diodes with large *r*-value disappear in Al/SAM/Al diodes; but the optical features related to the Me-BDT aggregates still remain. Transport properties of the mixed Au/SAM/Al devices at large *r*-values also show the low voltage *I-V* and DCS features, which are characteristic of aggregate-related COB in the gap, but only when the current is injected from the Au electrode; these features are not seen when the current is injected from the Al electrode. We believe that E_F(Al), being higher than E_F(Au) by ~1.0 eV does not cross the aggregate-related COB in the gap when the bias voltage is ramped up; and this explains the puzzle in the transport properties of Al/SAM/Au devices. We note that the low voltage aggregate-related response in SAM diodes is not unique to Au electrodes. In fact we obtained similar transport response also in Co/SAM/Co diodes, for which $E_F(\mathrm{Co}) \sim E_F(\mathrm{Au})$.[16]

ACKNOWLEDGMENTS

We acknowledge L. Wojcik for help with the chemical preparation; M. Delong, and C. Yang for help with the optical measurements; J. Shi and M. Zudov for the help with the *I-V* measurements; and A. Nitzan, E. Ehrenfreund, B. Shapiro, A. Pakoulev, M. Raikh and J. M. Gerton for useful discussions. This work was supported in part by the NSF NER 0507952, and DOE Grant No. FG-04ER46109 at the University of Utah.

[1] V. Burtman, A. S. Ndobe, and Z. V. Vardeny, J. Appl. Phys. **98**, 034314 (2005).
[2] M. A. Reed, C. Zhou, C. J. Muller, T. P. Burgin, and J. M. Tour, Science **278**, 252 (1997).
[3] Y. Selzer, M. A. Cabassi, T. S. Mayer, and D. L. Allara, Nanotechnology **15**, S483 (2004).
[4] J. R. Petta, S. K. Slater, and D. C. Ralph, Phys. Rev. Lett. **93**, 136601 (2004).
[5] M.-S. Hu, H.-L. I. Chen, C.-H. Shen, L.-S. Hong, B.-R. Huang, K.-H. Chen, and L.-C. Chen, Nat. Mater. **5**, 102 (2006).
[6] T. Dadosh, Y. Gordin, R. Krahne, I. Khivrich, D. Mahalu, V. Frydman, J. Sperling, A. Yacoby, and I. Bar-Joseph, Nature **436**, 677 (2005).
[7] W. Ho, J. Chem. Phys. **117**, 11033 (2002).
[8] C. Joachim, J. K. Gimzewski, and A. Aviram, Nature **408**, 541 (2000).
[9] C. D. Bain, E. B. Troughton, Y. T. Tao, J. Evall, G. M. Whitesides, and R. G. Nuzzo, J. Am. Chem. Soc. **111**, 321 (1989).
[10] R. Österbacka, C. P. An, X. M. Jiang, and Z. V. Vardeny, Science **287**, 839 (2000).
[11] V. Burtman, A. Zelichenok, and S. Yitzchaik, Angew. Chem., Int. Ed. **38**, 2041 (1999).
[12] D. Zaslavsky, A. Pakoulev, and V. Burtman, J. Phys. Chem. B **108**, 15815 (2004).
[13] H. Kuzmany, J. Fing, M. Mehring, and S. Roth, *Progress in Fullerene Research* (World Scientific, Singapore, 1994).
[14] S. Roth and D. Carroll, *One-Dimensional Metals: Conjugated Polymers, Organic Crystals, Carbon Nanotubes*, 2nd ed. (Wiley-VCH, Weinheim, 2004).
[15] D. Porath, A. Bezryanin, S. D. E. Vries, and C. Dekker, Nature (London) **403**, 635 (2000).
[16] V. Burtman, A. S. Ndobe, and Z. V. Vardeny, Solid State Commun. **135**, 563 (2005).
[17] Z. Mekhalif, J.-J. Pireaux, and J. Delhalle, Langmuir **13**, 2285 (1997).
[18] A. D. Vogt, T. Han, and T. P. Beebe, Langmuir **13**, 3397 (1997).
[19] C. E. D. Chidsey, Science **251**, 919 (1991).
[20] G. K. Ramachandran, T. J. Hopson, A. M. Rawlett, L. A. Nagahara, A. Primak, and S. M. Lindsay, Science **300**, 1413 (2003).
[21] H. Ron, H. Cohen, S. Matlis, M. Rapapport, and I. Rubinstein, J. Phys. Chem. B **102**, 9861 (1998).
[22] P. L. Schilardi, O. Azzaroni, and R. C. Salvarezza Phys, Phys. Rev. B **62**, 13098 (2000).
[23] A. Ulman, Chem. Rev. (Washington, D.C.) **96**, 1533 (1996).
[24] P. A. Lewis, Z. J. Donhauser, B. A. Mantooth, R. K. Smith, L. A. Bumm, K. F. Kelly, and P. S. Weiss, Nanotechnology **12**, 231 (2001).
[25] E. G. Emberly and G. Kirczenow, Phys. Rev. Lett. **87**, 269701 (2001).
[26] *Microscale Inorganic Chemistry: A Comprehensive Laboratory Experience* (Wiley, New York, 1991), p. 207.
[27] We have shown (Ref. 1) that the *I-V* characteristics and DCS spectra of SAM devices with *r*-values in the range $10^{-7} < r < 10^{-5}$ are similar to the device with $r = 10^{-6}$ discussed here. This indicates that the transport mechanism for all SSM SAM devices in this *r*-value range is basically the same.
[28] D. C. Müller, Ph.D. thesis, Swiss Federal Institute of Technology, Zurich, 2004.
[29] M. I. Slutskii, Semicond. Phys., Quantum Electron. Optoelectron. **7**, 68 (2004).
[30] R. Mehandru, S. Jang, S. J. Pearton, and F. Ren, in Proceedings of the 24th Army Science Conference Proceedings, Orlando, FL, 2004, Section N: Microelectronics and Photonics Technology (NP-04).
[31] A. Ulman, *An Introduction to Ultrathin Organic Films: From Langmuir-Blodgett to Self-Assembly* (Academic, New York, 1991).
[32] S. M. Sze, in *Physics of Semiconductor Devices*, 2nd ed. (Wiley, New York, 1981), Chap. 7.